Cell Proliferation

Cell Prolif. 2008, **41**, 875–893 doi: 10.1111/j.1365-2184.2008.00556.x

Lineage specific composition of cyclin D–CDK4/CDK6–p27 complexes reveals distinct functions of CDK4, CDK6 and individual D-type cyclins in differentiating cells of embryonic origin

V. Bryja*,†, J. Pacherník†, J. Vondráček*, K. Souček*, L. Čajánek‡,**, V. Horvath*, Z. Holubcová¶, P. Dvořák‡,§,¶ and A. Hampl‡,§,¶

**Institute of Biophysics, Academy of Sciences of the Czech Republic, Brno, Czech Republic, †Institute of Experimental Biology, Faculty of Science, Masaryk University, Brno, Czech Republic, ‡Center for Cell Therapy and Tissue Repair, Charles University, Prague, Czech Republic, §Department of Molecular Embryology, Institute of Experimental Medicine, Academy of Sciences of the Czech Republic, Prague, Czech Republic, and ¶Department of Biology, Faculty of Medicine, Masaryk University, Brno, Czech Republic*

Received 27 *August* 2007*; revision accepted* 15 *February* 2008

OnlineOpen: This article is available free online at www.blackwell-synergy.com

Abstract. *Objectives*: This article is to study the role of G_1/S regulators in differentiation of pluripotent embryonic cells. *Materials and methods*: We established a P19 embryonal carcinoma cell-based experimental system, which profits from two similar differentiation protocols producing endodermal or neuroectodermal lineages. The levels, mutual interactions, activities, and localization of G_1/S regulators were analysed with respect to growth and differentiation parameters of the cells. *Results and Conclusions*: We demonstrate that proliferation parameters of differentiating cells correlate with the activity and structure of cyclin A/E–CDK2 but not of cyclin D–CDK4/6–p27 complexes. In an exponentially growing P19 cell population, the cyclin D1–CDK4 complex is detected, which is replaced by cyclin D2/3–CDK4/6–p27 complex following density arrest. During endodermal differentiation kinase-inactive cyclin D2/D3–CDK4–p27 complexes are formed. Neural differentiation specifically induces cyclin D1 at the expense of cyclin D3 and results in predominant formation of cyclin D1/D2–CDK4–p27 complexes. Differentiation is accompanied by cytoplasmic accumulation of cyclin Ds and CDK4/6, which in neural cells are associated with neural outgrowths. Most phenomena found here can be reproduced in mouse embryonic stem cells. In summary, our data demonstrate (i) that individual cyclin D isoforms are utilized in cells lineage specifically, (ii) that fundamental difference in the function of CDK4 and CDK6 exists, and (iii) that cyclin D–CDK4/6 complexes function in the cytoplasm of differentiated cells. Our study unravels another level of complexity in G_1/S transition-regulating machinery in early embryonic cells.

Correspondence: V. Bryja, Department of Experimental Biology, Faculty of Science, Masaryk University, Kotlarska 2, 611 37 Brno, Czech Republic. Tel.: +420 532146226; Fax: +420 541211214; E-mail: bryja@sci.muni.cz; A. Hampl, Department of Biology, Faculty of Medicine, Masaryk University, Kamenice 5, 625 00 Brno, Czech Republic. Tel.: +420-549493514; Fax: +420-549498001; E-mail: ahampl@med.muni.cz

**Current address: Section of Molecular Neurobiology, Department of Medical Biochemistry & Biophysics, Karolinska Institutet, Stockholm, Sweden

INTRODUCTION

During development of multi-cellular organisms, cell lineages become specified, cells acquire unique cell fates, and they differentiate. Differentiation processes proceed in a balanced concerted way, with cell proliferation and cell death maintaining homeostasis of the entire organism. At least some differentiation processes can be effectively mimicked *in vitro* using pluripotent embryonic stem (ES) and embryonal carcinoma (EC) cells, which have their physiological *in vivo* counterparts in cells of pre-implantation embryos (Andrews *et al*. 2001; Smith 2001).

Cyclin-dependent kinases (CDKs), their activating and inhibiting partners – cyclins and CDK inhibitors (CKIs), are well recognized as essential regulators of cell proliferation. Their interactions, activities and functions as related to regulation of both progression of the cell cycle and maintenance of the quiescent state are well established (for reviews, see Sherr 1995; Sherr & Roberts 1999). Yet, irrespective of whether the cells reside in a developing embryo or in an adult organism, expression of individual cell cycle regulators of G_1 and S phases is significantly diverse, with individual cell types employing specific G_1/S cell cycle regulators to guarantee a balance between proliferation, quiescence, and/or maintenance of differentiation (for reviews, see Gao & Zelenka 1997; Nakayama & Nakayama 1998). In this study, mouse embryonal carcinoma cells (line P19) have been employed to address the question of how such molecular diversification develops during the earliest steps of differentiation that take place in the early embryo.

Up until now, several *in vitro* studies have been undertaken with the aim of understanding the role of cell cycle regulators in early differentiation; however, their results are not completely congruent (Savatier *et al*. 1995; Gill *et al*. 1998; Baldassarre *et al*. 1999; Li *et al*. 1999; Watanabe *et al*. 1999; Baldassarre *et al*. 2000; Glozak & Rogers 2001; Preclikova *et al*. 2002; Bryja *et al*. 2004b; Bryja *et al*. 2005). Still, as culture systems (monolayer versus three-dimensional), differentiation-inducing strategy/compounds, timing, cell density and other factors vary from study to study, controversies are likely to some extent, due to differences in experimental setup. Here, to overcome such limitations, we have introduced a simple experimental design that uses P19 EC cells, which profits from two different retinoic acid (RA)-based differentiation protocols, that in 4 days produce homogenous populations of primitive endodermal and primitive neuroectodermal cells, respectively. Importantly, it is also inherent to this setup that differentiation-associated changes to cell population growth, measured by cell density, DNA synthesis and distribution in cell cycle phases, are similar in both endodermal and ectodermal pathways. Experiments employing this design have led to the following findings: while cyclin A/E-CDK2 activity correlate with cell population growth parameters independently of differentiation status of cells, differences in cell fate are associated with existence of several types of molecular complex formed by D-type cyclins, CDK4, or CDK6 and p27. We assume that this molecular diversity mirrors distinct roles of (i) CDK4 and CDK6, and (ii) individual D-type cyclins, and that these molecules play a part in cell fate specification.

MATERIALS AND METHODS

Cell culture

P19 EC cells (ATCC no. CRL-1825) were cultured on gelatinized tissue dishes in Dulbecco's modified Eagle's medium (DMEM) containing 10% foetal calf serum, 0.05 mM β-mercaptoethanol,

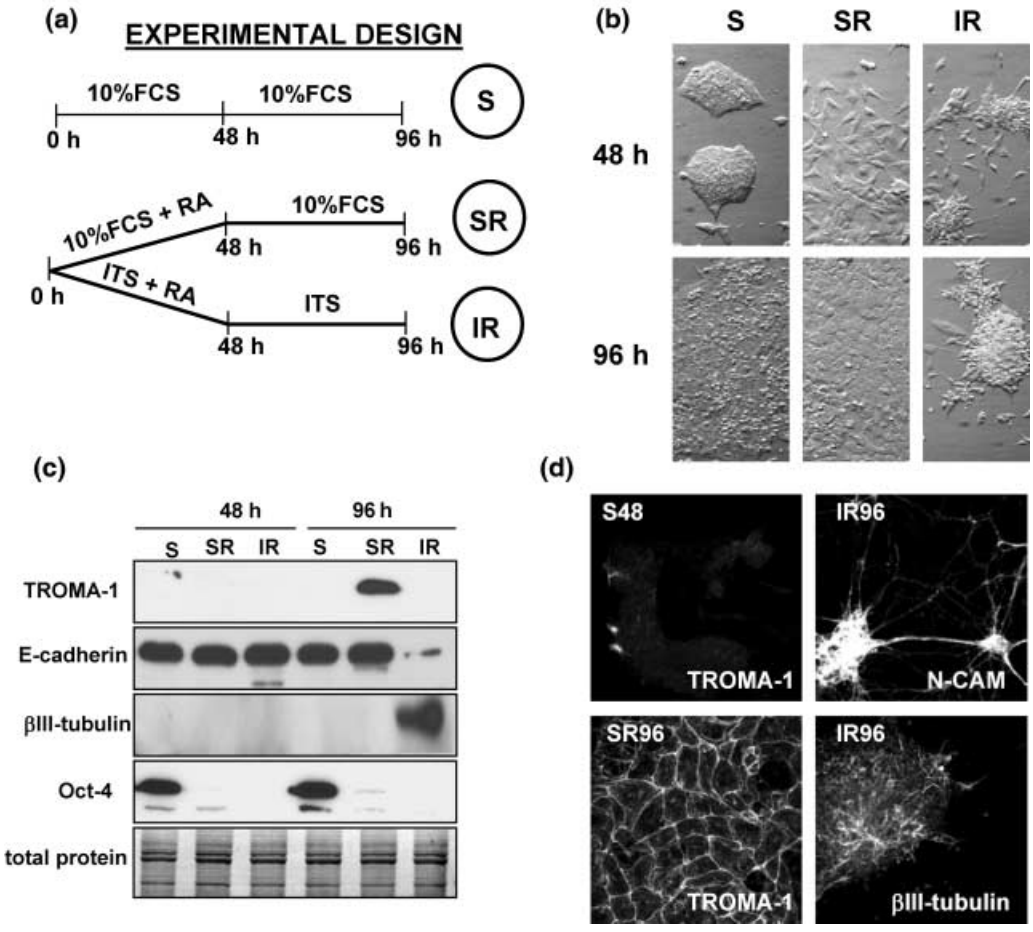

Figure 1. Characterization of differentiation protocols. (a) FCS, foetal calf serum; ITS, insulin-, transferrin- and selenium-supplemented medium (see the Material and Methods section); RA, retinoic acid. (b) The morphology and density of cells during the culture conditions outlined in (a) was monitored by phase contrast microscopy at 48 and 96 h. (c) Cells were differentiated according to protocols outlined in (a), and following 96 h of culture levels of cytokeratin endo A (TROMA-1), E-cadherin, βIII-tubulin and Oct-4 were determined by Western blotting. Total protein visualized using amidoblack staining is shown to demonstrate equal protein loading. (d) Following 96 h of culture, cells were fixed and stained for endodermal markers TROMA-1 (S and SR cells) and/or neural markers βIII-tubulin and N-CAM (IR cells).

100 IU/mL penicillin, and 0.1 mg/mL streptomycin. Mouse ES cells (line 10) and conditions for their culture have been described previously (Bryja *et al*. 2004b). To initiate differentiation, cells (5×10^3 per cm^2) were seeded onto gelatinized tissue culture dishes 12 h before application of experimental conditions. The cells were then cultured for 48 h in DMEM containing 10% foetal calf serum or in DMEM/F-12 (1 : 1) media supplemented with insulin–transferrin–selenium supplement (ITS) and antibiotics (further referred to as ITS medium) (all Gibco-Invitrogen, Carlsbad, CA, USA) either in the presence or absence of 0.5 μM RA (Sigma-Aldrich, St. Louis, MO, USA). RA was then removed from the respective cultures and all cell populations were grown for another 48 h until the experiments were ended at 96 h (see Fig. 1a, for the schematic diagram of culture conditions).

Cell population growth rate

Increases in absolute cell number and total cell protein were used as a measure of cell population growth. Total cell number of P19 cells growing and/or differentiating on 6-well plates, according to protocols described in Fig. 1a, were determined using a haemocytometer. Total cell protein was determined as follows. Cells on culture dishes were washed twice with phosphate-buffered saline (PBS; pH 7.2) and were lysed in 100 mM Tris-HCl (pH 6.8) buffer containing 20% glycerol and 1% sodium dodecyl sulfate (SDS). Protein concentrations, determined using a DC protein assay kit (Bio-Rad, Hercules, CA, USA), were used to calculate total amount of protein per dish.

Analysis of cell cycle distribution and DNA synthesis

For analysis of DNA synthesis, cells were labelled with 10 μM 5-bromo-2′-deoxyuridine (BrdU) for 60 min, under standard culture conditions (37 °C, 5% CO_2, 95% humidity). After labelling, cells were trypsinized then fixed in 70% ethanol at 4 °C overnight. Cell cycle distribution and proportion of BrdU-positive cells were quantified using flow cytometry (argon ion laser, 488 nm excitation, FACSCalibur – Becton Dickinson, San Jose, CA, USA) essentially as described previously (Bryja *et al*. 2004b).

Real-time RT-PCR

Levels of mRNA for $p27^{Kip1}$, cyclin D1, cyclin D2 and cyclin D3 were determined by real-time quantitative RT-PCR using TaqMan® Gene Expression Assays (Mm00438167_g1, Mm00432359_m1, Mm00438071_m1, Mm01612362_m1, respectively; Applied Biosystems, Foster City, CA, USA). Total RNA was isolated from cells using the RNeasy mini kit (Qiagen, Valencia, CA, USA). Amplification of the samples (200 ng of total RNA per reaction) was carried out in duplicate, using QuantiTect Probe RT-PCR kit (Qiagen) according to manufacturer's instructions. All amplifications were run on a Rotor-Gene™ thermal cycler (Corbett Research, Sydney, Australia), using the following program: reverse transcription at 50 °C for 30 min, initial activation step at 95 °C for 15 min, followed by 40 cycles at 94 °C for 15 s and 60 °C for 60 s. Gene expression for each sample was expressed in terms of the threshold cycle (C_t) normalized to glyceraldehyde 3-phosphate dehydrogenase (GAPDH) (ΔC_t), as determined using TaqMan® Rodent GAPDH Control Reagents (Applied Biosystems). ΔC_t values were then compared between control samples (cells grown for 48 h) and samples from treated cells, to calculate $\Delta\Delta C_t$ [ΔC_t (control) – ΔC_t (test sample)]. Final comparison of transcript ratios between samples is given as $2^{-\Delta\Delta Ct}$ (Livak & Schmittgen 2001).

Western blot analysis

Cells on culture dishes were washed twice with PBS (pH 7.2), lysed in 100 mM Tris-HCl (pH 6.8) containing 20% glycerol and 1% SDS, and were analysed by SDS-polyacrylamide gel electrophoresis (PAGE) as described previously (Bryja *et al*. 2004b). Antibodies used were as follows: mouse monoclonal antibody to cyclin D1 (sc-450), rabbit polyclonal antibodies to CDK6 (sc-177), cyclin E (sc-481), poly(ADP-ribose) polymerase (PARP) (sc-7150) and Oct-4 (sc-9081), and goat polyclonal antibodies to CDK2 (sc-163-G), CDK4 (sc-601-G), and lamin B (sc-6217) were purchased from Santa Cruz Biotechnology (Santa Cruz, CA, USA); mouse monoclonal antibody to mouse p27 (K25020) was purchased from Transduction Laboratories (Lexington, KY, USA); mouse monoclonal antibodies specifically recognizing cyclin A (Ab-1, E23) and cyclin D2 (Ab-4, DCS-3.1 + DCS-5.2) (Bartkova *et al*. 1995) were purchased from Neomarkers (Fremont, CA, USA); mouse monoclonal antibody specifically recognizing part of the C-terminal of human cyclin D3, which cross-reacts with the mouse homologue (DCS-22)

(Bartkova *et al*. 1996), was generously provided by Dr. Jiri Lukas (Danish Cancer Society, Copenhagen, Denmark). Mouse monoclonal antibody against human neuron-specific class III β-tubulin isotype, which cross-reacts with the mouse homologue (TU-20) was generously provided by Dr. Pavel Draber (Institute of Molecular Genetics, Prague, Czech Republic). The TROMA-1 hybridoma developed by Drs. P. Brulet and R. Kemler was obtained from the Developmental Studies Hybridoma Bank, developed under the auspices of the National Institute of Child Health and Development, and was maintained by the University of Iowa, Department of Biological Sciences (Iowa City, IA, USA). After immunodetection, each membrane was stained using amidoblack to confirm equal protein loading.

Immunoprecipitation and kinase assays

For these assays, cells were extracted in ice-cold lysis buffer for 30 min [50 mM Tris-HCl (pH 7.4), 150 mM sodium chloride, 0.5% Nonidet P-40, 1 mM ethylenediaminetetraacetic acid, 0.1 mM dithiothreitol, 50 mM sodium fluoride, 8 mM β-glycerophosphate, 100 mM phenylmethylsulphonyl fluoride (PMSF), 1 μg/mL leupeptin, 1 μg/mL aprotinin, 10 μg/mL soybean trypsin inhibitor, 10 μg/mL tosylphenylalanine chloromethane], and further processed essentially as described previously (Bryja *et al*. 2004b). Briefly, extracts were cleared by centrifugation at 15 000 ***g*** for 5 min at 4 °C and were stored at −80 °C until use. After thawing, protein concentrations were determined using a DC protein assay kit (Bio-Rad). Extracts were incubated with appropriate antibodies for 1 h, on ice. The following antibodies were used: sc-601-G against CDK4, sc-163-G against CDK2, sc-177 against CDK6, sc-751 against cyclin A, and sc-481 against cyclin E (all purchased from Santa Cruz Biotechnology). Immunoprecipitates were collected on Protein G agarose beads by overnight rotation, washed four times with lysis buffer, re-suspended in 2× Laemmli sample buffer, and were subjected to SDS-PAGE followed by Western blot analysis. To control for specificity of the immunoprecipitation reaction, the control sample containing only cell lysate and G protein-coupled beads, but no antibody, was included in each set of immunoprecipitated samples (no antibody control). For kinase assays, immunoprecipitates were prepared as above, except that the last two washes were performed using kinase assay buffer [50 mM N-(2-hydroxyethyl) piperazine-N′-(2-ethanesulfonic) acid (HEPES), pH 7.5; 10 mM $MgCl_2$; 10 mM $MnCl_2$; 8 mM β-glycerophosphate; 1 mM dithiothreitol]. For CDK2, kinase reactions were carried out for 30 min at 37 °C in a total volume of 25 μL in kinase assay buffer supplemented with 100 μg/mL histone H1 (type III-S) and 40 μCi/mL [^{32}P]ATP. For CDK4, kinase reactions were carried out for 30 min at 30 °C in a total volume of 25 μL in kinase assay buffer supplemented with 160 μg/mL GST-pRb (type III-S) and 40 μCi/mL [^{32}P]ATP. Reactions were terminated by addition of 2× Laemmli sample buffer and each reaction mix was subjected to SDS-PAGE and autoradiography. Two controls complemented each set of kinase reactions: no antibody control and no substrate control. When required, intensities of signals were assessed by densitometry using Intelligent Quantifier software (BioImage, Ann Arbor, MI, USA).

Isolation of nuclear and cytoplasmic fractions

Cells were washed in PBS and dry frozen at −70 °C for further use. Following freezing, cells were scraped in TKM buffer (50 mM Tris-HCl, pH 7.4, 5 mM $MgCl_2$; 25 mM KCl; 100 mM PMSF; 1 μg/mL leupeptin; 1 μg/mL aprotinin; 10 μg/mL soybean trypsin inhibitor; 10 μg/mL tosylphenylalanine chloromethane), sonicated (10 s, 25 W), and fractionated by centrifugation (10 min, 1000 ***g***, 4 °C). When necessary, the supernatant, representing the cytoplasmic fraction, was precipitated using trichloroacetic acid. Both pellet and precipitate were then dissolved in 100 mM Tris-HCl (pH 6.8) containing 20% glycerol and 1% SDS. Protein in each fraction was quantified, and equal amounts of total protein were analysed by Western blotting.

Immunocytochemistry and confocal microscopy

Expression of differentiation markers and subcellular localization of cyclins and CDKs were determined by indirect immunofluorescence using the following antibodies: rat monoclonal antibody to mouse endoderm-specific cytokeratin endo A (TROMA-I, Developmental Studies Hybridoma Bank, University of Iowa), mouse monoclonal antibody to cat HNK-1/N-CAM, which cross-reacts with the mouse homologue (VC1.1, Sigma), and mouse monoclonal antibody to human neurone-specific class III β-tubulin isotype, which cross-reacts with the mouse homologue (TU-20, provided by Pavel Dráber, Institute of Molecular Genetics, Prague, Czech Republic). Antibodies to cyclin D1 (sc-450), CDK4 (sc-260), and cyclin A (sc-751) were from Santa Cruz Biotechnology and antibody to CDK6 (Ab4) was from Neomarkers. Cells were fixed for 30 min on ice in ethanol/acetic acid (95% ethanol, 1% acetic acid, for differentiation markers) or in 4% paraformaldehyde (for cell cycle regulators), then samples were stepwise rehydrated, quenched with 1% bovine serum albumin in PBS for 1 h at room temperature, incubated with the appropriate primary antibody (overnight at 4 °C) and FITC-conjugated secondary (1 h at room temperature) antibodies, and mounted using Mowiol (Sigma). Cells were observed either under an Olympus BX-60 epifluorescence microscope (Olympus, Prague, Czech Republic) or were scanned using an Olympus Fluoview 5000 confocal laser scanning microscope.

Statistics

Data were expressed as means ± standard deviations and were analysed using Student's *t*-test or by one-way analysis of variance (ANOVA) followed by the Tukey's range test (Fig. 2c). A P value of less than 0.05 was considered to be significant.

RESULTS

Characterization of the experimental model

P19 EC cells were differentiated according to two RA-based differentiation protocols (Fig. 1a, schematic). Cells growing in serum-containing medium or in serum-free ITS medium were first treated with RA for 48 h. Then, they were cultured in the respective media without RA for another 48 h, thus establishing two cell groups further referred to as SR (serum + RA) and IR (ITS + RA) cells, respectively. It was typical for SR cells to form monolayers of flat cells (Fig. 1b), to express markers of extraembryonal endoderm such as TROMA-1 (Fig. 1c,d), and to lack markers of undifferentiated and/or neural cells (Fig. 1c and not shown). In contrast, IR cells adopted neural morphology (Fig. 1b) and started to express neural markers, for example neural specific class III β-tubulin or N-CAM (Fig. 1c,d), while lacking both the endodermal marker TROMA-1 and the marker of undifferentiated cells Oct-4 (Fig. 1c,d). Control cells were cultured for 96 h in serum-containing medium (undifferentiated P19 EC cells, further referred to as S cells). Control cells at 48 h (S48) were fully proliferative and undifferentiated (as repeatedly judged by Oct-4 expression) and thus represent the basic control. More detailed characterization of the outcomes of SR and IR differentiation protocols has been provided previously (Pachernik *et al*. 2005).

Cell population growth and cell cycle characteristics

Because population growth- and differentiation-related metabolisms of cell cycle regulators were to be addressed in this study, it was necessary to first define cell population growth and cell cycle characteristics of differentiating P19 cells. As determined by both total protein (Fig. 2a) and total cell number (Fig. 2b), treatment with RA resulted in population growth retardation,

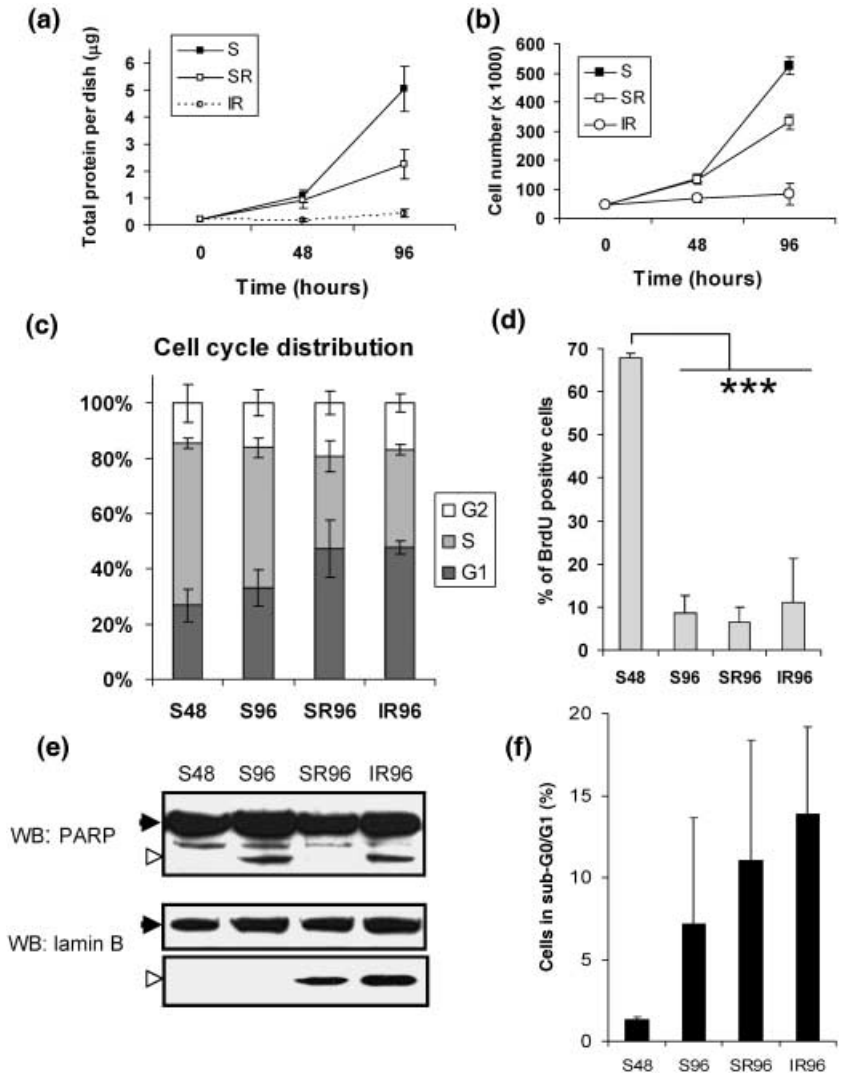

Figure 2. Cell population growth and cell cycle properties. Cells were cultured according to protocols outlined in Fig. 1a, and at 48 and 96 h of culture population growth and cell cycle properties were determined. Total protein per dish (a) and total number of cells per dish (b) were quantified and used as a measure of cell population growth. Mean and standard deviations from three independent replicates are shown. (S cells – full square; SR cells – open square; IR cells – open circle). (c) Percentage of cells in individual cell cycle phases was determined by flow cytometry (mean ± SD, $n = 6$). (d) Cells were labelled with BrdU for metabolic studies and subsequently they were stained with propidium iodide and FITC-conjugated anti-BrdU antibody; then, they were scored by flow cytometry. The percentage of BrdU positive cells indicated as the mean ± SD from three independent replicates is shown. (e) Cleavage of PARP and lamin B was determined by Western blotting (full arrowheads – full length protein; open arrowheads – cleaved fragment). (f) Proportion of cells at sub-G_0/G_1 population (mean ± SD, $n = 3$), which corresponds to apoptotic cells, was determined by FACS. ***$P < 0.001$.

which was more pronounced in IR cells. Distribution of cells in G_1, S and G_2 phases was then determined for all three culture protocols, by flow cytometry (Fig. 2c). A significant decrease in numbers of cells in S phase took place after induction of differentiation (S48 versus SR96/IR96; $P < 0.001$, One-way ANOVA) and also with increased cell density (S48 versus S96; $P < 0.05$). Flowcytometric counting of BrdU-pulse-labelled cells (Fig. 2d) showed that 60–70% of S48 control cells incorporated BrdU into their DNA, whereas at the 96 h time point only, around 10% of cells retained BrdU in S96, SR and IR. Clearly, increased cell density and RA-induced differentiation both caused inhibition of DNA synthesis under our culture conditions. A high proportion of S96 cells in S phase suggests that a density-dependent slowdown of DNA synthesis and subsequent S phase arrest was a major mechanism responsible for reduction in proliferation in undifferentiated P19 EC cells, as was shown recently for mouse ES cells (Jirmanova *et al*. 2005; Andäng *et al*. 2008). In contrast, both SR and IR cells accumulated in G_1 phase at the expense of in S phase, suggesting that G_1/S transition was affected. Importantly, SR and IR cells were indistinguishable from each other based on cell cycle distribution/proliferation characteristics. As an additional parameter, we analysed the level of apoptosis using three apoptotic markers – cleavage of PARP, cleavage of lamin B, and proportion of cells in sub-G_0/G_1. We could detect cleavage of caspase substrates PARP and lamin B clearly (Fig. 2e) and increased number of cells in sub-G_0/G_1 population in S96, SR96 and IR96 cells, as determined by fluorescence-activated cell sorter (FACS) analysis (Fig. 2f). Interestingly, PARP was cleaved mainly in S96 and IR96 cells, whereas lamin B was cleaved mainly in SR96 and IR96 cells. PARP and lamin B are substrates of distinct caspases (Slee *et al*. 2001), and different patterns of their cleavage suggest that the mechanisms of apoptotic activation in S96, SR96 and IR96 cells may differ.

Structure and kinase activity of cyclin A/E-CDK2-p27 complexes during differentiation

CDK2 and its regulatory partners, cyclins A and E, and appropriate CKIs are major drivers of G_1/S transition and S-phase progression. We have analysed levels, mutual interactions, and kinase activities of cyclins A and E, CDK2, and p27 (the only CKI showing detectable levels in P19 cells; Fig. 3). Cyclin E-associated kinase activity dropped both by induction of differentiation (SR/IR) and with increasing cell density (S96), which is likely due to a combination of increased binding of p27 and down-regulation of cyclin E. Cyclin A showed a more complex pattern, which was characterized by decreased cyclin A-associated kinase activity and increased association with p27 in differentiated cells (SR96/IR96). Interestingly, increased density of S96 cells resulted in increased level of cyclin A and cyclin A/CDK2 activity, despite higher association with p27. Because S96 cells did not incorporate BrdU (Fig. 2c), it is possible that cyclin A/CDK2 complex had an additional function in S96 cells. In all cultures other then S96, however, activity of CDK2 correlates well with binding of its activating and inhibiting partners and matches observed growth characteristics of the cells (Fig. 2).

Levels of D-type cyclins during cell differentiation

Along with CDK2, CDK4 and CDK6 with their partner D-type cyclins were involved in regulation of G_1/S transition. As shown in Fig. 4a, only cyclin D1 was expressed in significant levels in fully proliferating undifferentiated P19 cells (S48), although a minute amount of cyclin D2 was also present. When differentiation was induced, both cyclin D2 and cyclin D3 became up-regulated (Fig. 4a). Prolonged culture lead also to up-regulation of cyclin D3 in undifferentiated S96 cells, suggesting that not only RA treatment but also other signals (most likely increased cell density), may induce expression of D-type cyclins in P19 cells. Previously, we have shown that in differentiated cells, D-type cyclins accumulate due to stabilization by binding partners and not due to changes in their transcription (Bryja *et al*. 2004a). To resolve whether or not the changes in levels of

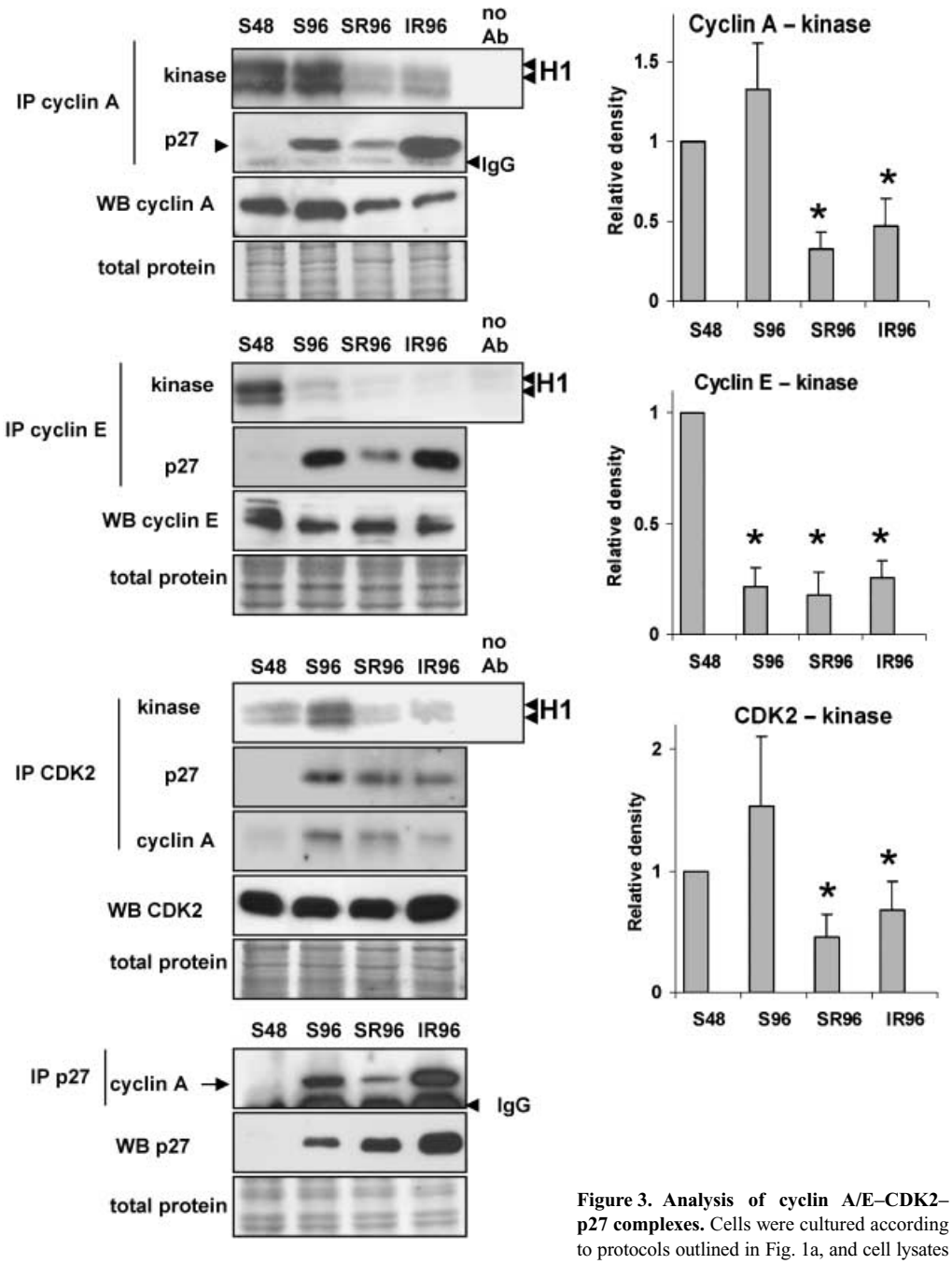

Figure 3. Analysis of cyclin A/E–CDK2–p27 complexes. Cells were cultured according to protocols outlined in Fig. 1a, and cell lysates were used to immunoprecipitate cyclin A, cyclin E, CDK2 and p27. In cyclin- and CDK2-immunoprecipitates kinase activities towards histone H1 were determined by autoradiography and three independent replicates were quantified by densitometry. Graphs represent means ± SDs of autoradiographic signal normalized to S samples at 48 h. Quantity of p27 in cyclin A, cyclin E and CDK2 immunoprecipitates and the amount of cyclin A in CDK2 and p27 immunoprecipitates were determined by Western blotting. Total amount of cyclin A, cyclin E, CDK2 and p27 as determined by Western blotting and total protein level as determined by amidoblack staining are also presented. Data are representative of at least three independent replicates.

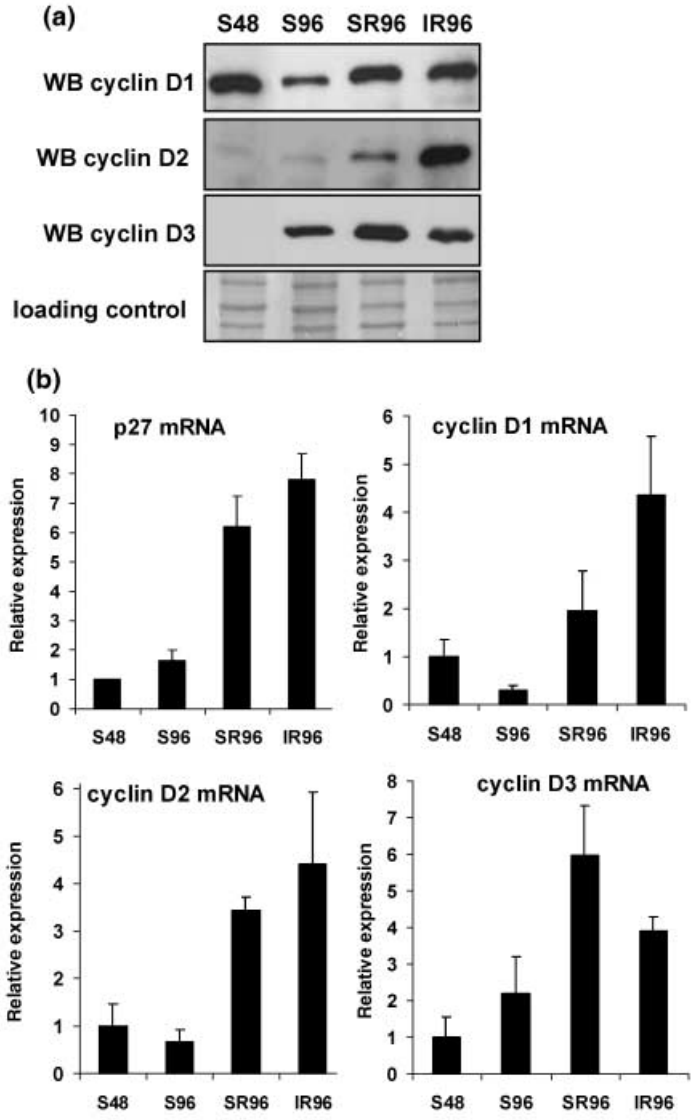

Figure 4. Expression of D-type cyclins. Cells were cultured according to protocols outlined in Fig. 1a. (a) Amounts of cyclins D1, D2 and D3 in protein samples were quantified by Western blotting. Data are representative of four independent replicates. (b) Expression of mRNA coding for p27, cyclins D1, D2 and D3 was quantified using quantitative real-time RT-PCR. Data represent means ± SDs of four independent replicates.

D-type cyclins and p27 were due to increased levels of transcripts, we have determined the mRNA levels by real-time quantitative RT-PCR (Fig. 4b). Amounts of transcripts coding for cyclins D and p27 matched well changes in the respective protein levels, suggesting that D-type cyclins and p27 were regulated during differentiation primarily via transcription mechanisms. Only cyclin D1 showed more complex regulation with low quantities of protein in differentiated cells despite high level of its mRNA. Importantly, based on the obvious lack of correlation between levels of mRNA for individual D-type cyclins and cell growth characteristics, we

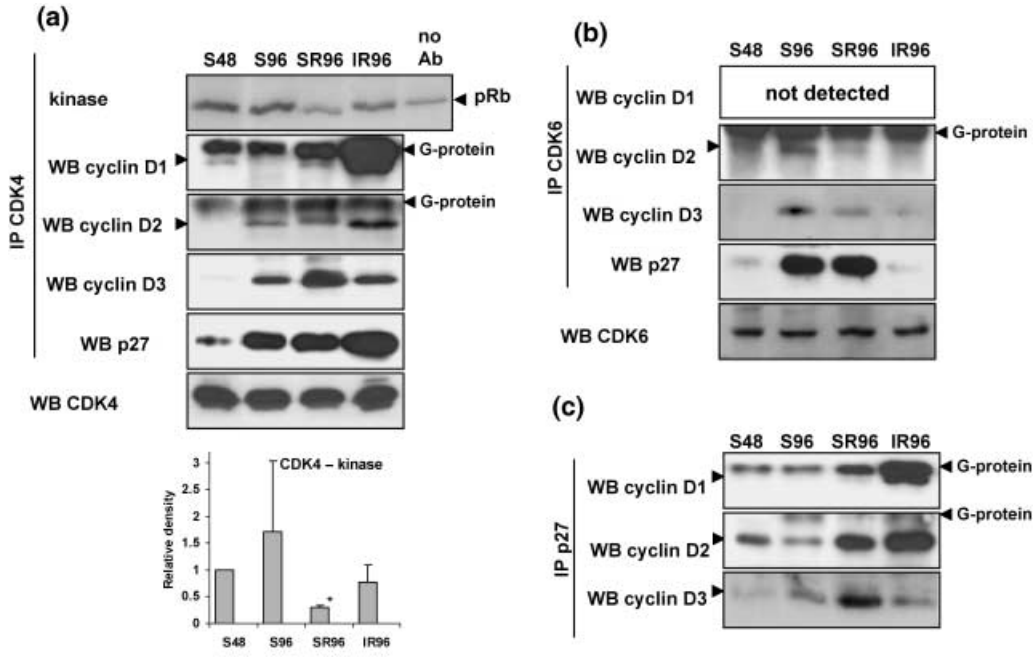

Figure 5. Analysis of cyclin D–CDK4/6–p27 complexes. Cells were cultured according to protocols outlined in Fig. 1a, and cell lysates were analysed. (A) In CDK4 immunoprecipitates, kinase activities to GST-pRb were determined by autoradiography and three independent replicates were quantified by densitometry. Graphs represent means ± SDs of autoradiographic signals normalized to S-phase samples at 48 h. Amounts of cyclin D1, cyclin D2, cyclin D3 and p27 in CDK4 immunoprecipitates, as well as total level of CDK4, were determined by Western blotting. (b) Quantities of cyclin D2, cyclin D3 and p27 in CDK6 immunoprecipitates, as well as total amount of CDK6, were determined by Western blotting. (c) Samples were immunoprecipitated by p27-specific antibody and levels of cyclin D1, cyclin D2 and cyclin D3 bound to p27 were determined by Western blotting. Data in (a–c) are representative of at least three independent replicates.

hypothesize that in differentiating P19 cells these cyclins play role(s) other than regulation of cell cycle progression.

Activity and binding partners of CDK4 and CDK6 during differentiation

In the next step, we determined to what extent changes in levels of D-type cyclins translated into composition and activity of complexes involving CDK4 and CDK6. Both CDK4 and CDK6 proteins were present in P19 cells with their total quantities not changing during differentiation (Fig. 5a,b). Interestingly, there were major differences among D-type cyclins in their association with CDK4. While in fully proliferating undifferentiated P19 cells (S48) cyclin D1 was the only cyclin bound to CDK4, significant physical interaction of CDK4 with cyclins D2 and D3 was observed in cells induced to differentiate by RA. Specifically, the following cyclins had undergone the most prominent increase in binding to CDK4: (i) cyclins D2 and D3 in undifferentiated S cells, (ii) cyclin D3 in endodermal (SR) cells, and (iii) cyclins D1 and D2 in neural (IR) cells.

Despite our inability to detect measurable CDK6-associated kinase activity, there were clear partnerships of this molecule with some D-type cyclins and also with p27 (Fig. 5b). Interestingly, binding of D-type cyclins to CDK6 was completely different from their association to CDK4. In undifferentiated, proliferating S48 cells, CDK6 associated with only small amounts of cyclin D2 and p27. In contrast, growth-arrested S96 cells were characterized by high levels of cyclins D2

and D3 interacting with CDK6; however, such interactions were much less pronounced in cells differentiating into endodermal (SR) and neural (IR) lineages. Strong physical interaction between CDK6 and p27 was detected in S96 and SR96 cells. No interaction of cyclin D1 with CDK6 was observed under any condition. To complement the analysis, we also determined the portions of D-type cyclins that physically interacted with p27. Cyclin D1 bound to p27 in IR96 cells (Fig. 5), cyclin D2 bound to p27 in a pattern corresponding well to the total amount of cyclin D2, and cyclin D3 bound to p27, mainly in dense, serum-containing cultures (S96 and SR96 cells). Taking all these data together, CDK4 associated with p27 and D-type cyclin partners mainly during differentiation of P19 cells, although such interactions were clearly specific for individual D-type cyclins. In contrast, complexes involving CDK6 and its partners developed predominantly in cells that were approaching confluence (S96 and SR96). Importantly, although D-type cyclins associated with CDK4 during differentiation, neither CDK4-associated kinase activity nor cell population growth was stimulated in differentiating cells.

Localization of p27 and D-type cyclins in differentiating cells

Cyclin-CDK complexes phosphorylate their targets, which then further regulate cell cycle progression. The majority of these events occur in nucleus. In this study, we have shown that changes in levels of D-type cyclins were not linked to cell cycle characteristics of differentiating P19 cells. Therefore, we hypothesized that specific subcellular localization of certain members of cell cycle-regulating machinery may be responsible for absence of the expected link. To address this issue, we employed immunocytochemistry to visualize subcellular localization of cyclin A, cyclin D1, CDK4 and CDK6 *in situ* in S48 (undifferentiated), SR96 and IR96 cells. As shown in Fig. 6a, cyclin A was predominantly nuclear under all conditions. In contrast, although cyclin D1, CDK4 and CDK6 were mostly nuclear in undifferentiated cells (S48), they all appeared in cytoplasm following differentiation to endodermal (SR96) and/or neural (IR96) lineages. Interestingly, in neural IR cells, both CDK4 and CDK6 were heavily associated with neurite outgrowths. To complement immunohistochemical analysis, cell lysates of differentiated cells were separated into nuclear and cytoplasmic fractions, and the efficiency of this separation process was confirmed by including analysis of cytoplasmic α-tubulin, a component of nuclear membrane lamin B, and chromating binding protein HP1α. As shown in Fig. 6b, all D-type cyclins and p27 were predominantly cytoplasmic. These localization data fit the general scenario well, in which the major cell cycle driving force in pluripotent embryonic cells is represented by cyclin A–CDK2–p27 complexes, whereas cytoplasmic CDK4/6, in association with D-type cyclins and p27, predominantly have other function in differentiating cells.

Dynamics of expression, binding and localization of cell cycle regulators in mouse ES cells

To further address the significance of the behaviour of cell cycle regulators observed here in P19 cells, untransformed pluripotent mouse embryonic stem cells (mESCs) were also subjected to similar analyses. We were not successful in transferring the neural differentiation protocol (IR) to mESCs, mainly because high cell death was associated with given treatments to mESCs (not shown). Yet, the endodermal differentiation protocol (SR) proved to be fully applicable to mESCs and produced relevant data. As shown in Fig. 7a, expression patterns of D-type cyclins and p27 did not differ from those observed in differentiating P19 cells. Importantly, endodermal differentiation was accompanied by remodelling of protein complexes involving CDK4 (Fig. 7b). In undifferentiated mESCs (S48), CDK4 predominantly bound cyclin D1, which was replaced during progressing differentiation by cyclins D2 and D3 together with p27. These expression and interaction patterns closely resemble behaviour of the cell cycle regulators in P19 cells, differentiating under identical conditions. Interestingly, similarly to P19 cells, cyclin D/CDK4/p27 complexes in differentiating mESCs

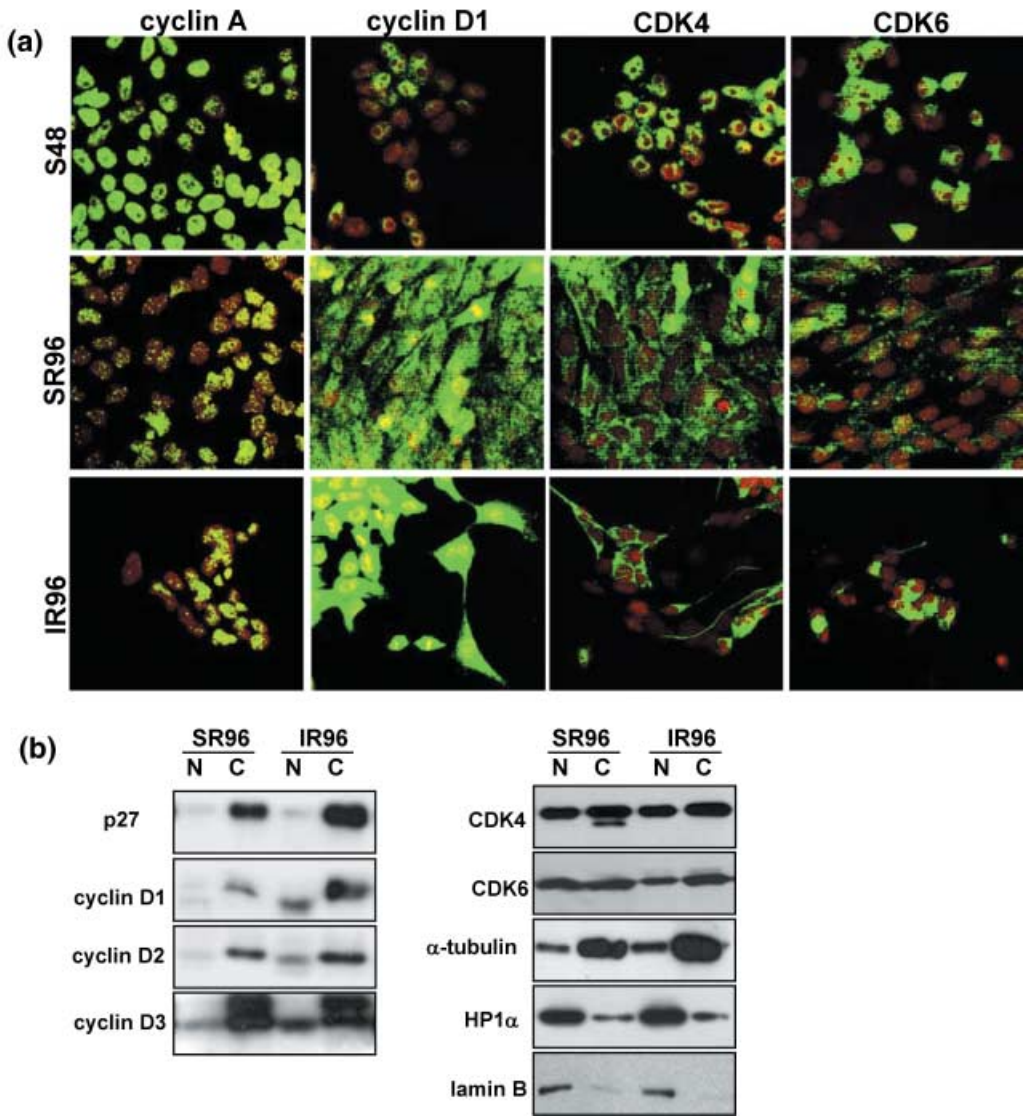

Figure 6. Intracellular localization of regulators of G_1/S transition. (a) Subcellular localization of cyclin A, cyclin D1, CDK4 and CDK6 as determined by immunocytochemistry (green) in undifferentiated cells (S48) and in cells differentiated into endodermal (SR96) and neural (IR96) lineages. Nuclei were visualized by counterstaining with propidium iodide. All scans have been acquired using identical settings of the confocal microscope. (b) Cells were grown according to protocols outlined in Fig. 1a, and at 96 h of culture cell lysates were separated into nuclear and cytoplasmic fractions. Amounts of p27, D-type cyclins, CDK4 and CDK6 in nuclear (N) and cytoplasmic (c) fractions were quantified by Western blotting. To demonstrate efficiency of separation, levels of control proteins localized predominantly to cytoplasm (α-tubulin) and nucleus (lamin B, HP1α) were also analysed by Western blotting.

were likely to be localized in the cytoplasm as indicated by cytoplasmic localization of individual D-type cyclins, CDK4 and p27 (Fig. 7c). Taken together, metabolism of cell cycle regulators, although here determined in detail primarily using P19 EC cells, is very likely characteristic for pluripotent cells of embryonic origin rather than only for transformed EC cells.

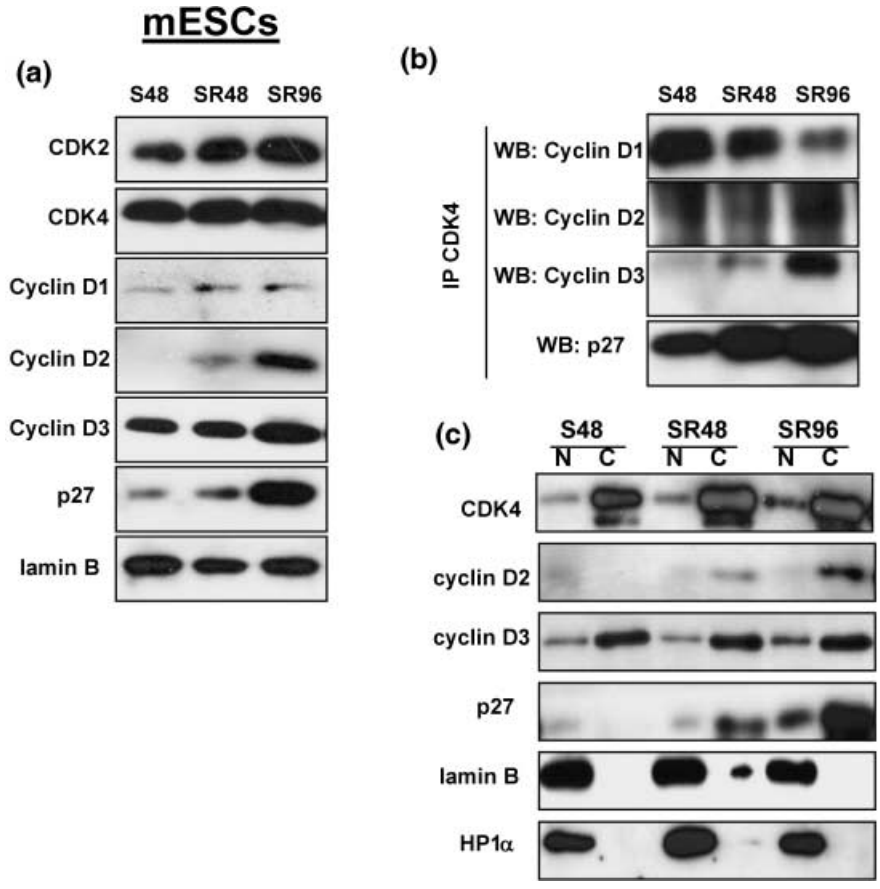

Figure 7. Analysis of cyclin D–CDK4/6–p27 complexes in mouse embryonic stem cells (mESCs). mESCs (S48) were cultured according to SR protocol outlined in Fig. 1a for 48 (SR48) and 96 h (SR96). (a) Expression of CDK2, CDK4, cyclin D1, cyclin D2, cyclin D3 and p27 were determined by Western blotting; lamin B was used as a loading control. (b) Cell lysates were subjected to immunoprecipitation using anti-CDK4 antibody (IP CDK4) and amount of cyclins D1, D2, D3, and p27 bound to CDK4 in immunoprecipitates was analysed by Western blotting. (c) Cell lysates were subjected to nucleo/cytoplasmic separation and levels of CDK4, cyclin D2, cyclin D3 and p27 in nuclear (N) and cytoplasmic (c) fractions were analysed by Western blotting. Nuclear proteins lamin B and HP1α were used as loading and separation efficiency controls. Data in (a–c) are representative of three independent replicates.

DISCUSSION

Cell type- and tissue-specific expressions of cyclins and CKIs during development and in the adult are believed to not only underlie differences in cell cycling parameters but also to participate in promoting differentiation and/or maintenance of the differentiated state. The ultimate aim of this study was to investigate the link between metabolism of key members of the cell cycle-regulating machinery and lineage determination, in differentiating pluripotent cells of embryonic origin. To do so, two differentiation protocols were implemented, which produced cells of two different phenotypes: endodermal (positive for TROMA-1) and neural (positive for neural specific class III β-tubulin). Analyses described here have led to two major revelations. First, the cell cycle characteristics of P19 cells and their differentiated progeny correlated well with activity of

CDK2. Moreover, activity of CDK2 correlated with cyclin A- and cyclin E-associated kinase activity, as well as with association with CDK inhibitor p27. Second, amounts of D-type cyclins and their physical interactions with CDK4 were elevated in the conditions which did not support proliferation. Moreover, complexes of D-type cyclins with CDK4/6, which are distinct depending on differentiation program, were localized predominantly in cytoplasm, contrasting with the nuclear localization of complexes involving cyclin A and CDK2. Taken together, these data strongly suggest that although cyclin A/E–CDK2–p27 complex regulates progression of the cell cycle in differentiating P19 cells, major role of cyclin D–CDK4 complexes in these embryonic cells differed from the regulation of entry into S phase. It should, however, be noted that any pro-differentiation function of cyclin D–CDK4/6–p27 complexes was not in conflict with their function in regulation of G_1/S transition. It is possible that subcellular localization represents a mechanism of how these independent functions were realized and regulated.

It has been shown that although cells are able to proliferate in the absence of both CDK4/6 kinases (Malumbres *et al*. 2004) and D-type cyclins (Kozar *et al*. 2004), differentiation in D-cyclin-null embryos is often affected (Fantl *et al*. 1995; Sicinski *et al*. 1995; Chellappan *et al*. 1998; Huard *et al*. 1999; Ciemerych *et al*. 2002). Our screen identifies cyclin D2, cyclin D3 and p27 as the molecules that become expressed and stay elevated when EC and mESC cells are induced to differentiate. Instead, bimodal expression was typical for cyclin D1 (with this cyclin being high in undifferentiated cells), and after transient decrease being up-regulated again, but only in the neural lineage. Obviously, the coordinated increase of p27 and cyclin D2 and/or D3 during differentiation was not an uncommon phenomenon, as it has been widely described using other differentiation models (Savatier *et al*. 1995; Gill *et al*. 1998; Baldassarre *et al*. 1999; Li *et al*. 1999; Watanabe *et al*. 1999; Baldassarre *et al*. 2000; Glozak *et al*. 2001; Preclikova *et al*. 2002; Bryja *et al*. 2004b; Bryja *et al*. 2005). In the present study, however, detailed analysis of the dynamics of a composition of cyclin D–CDK4/6–p27 complex unravelled important differences, not only in a utilization of individual D-type cyclins but also in the roles of CDK4 and CDK6, respectively. As indicated in the schematic diagram (Fig. 8a), undifferentiated, exponentially growing cells (S48) mostly contained cyclin D1 associated with CDK4 and a low level of cyclin D2 complexed with CDK6. Although p27 was detected, the level of this regulator was very low in undifferentiated P19 cells. In 2 further days, when cells cultured under non-differentiating conditions reached confluence (S96), p27, cyclin D2 and cyclin D3 were induced and they bound mainly to CDK6 and to CDK4. Simultaneously, expression of cyclin D1 became reduced and its binding to CDK4 was abolished.

In contrast to the molecular pattern typical for cultures of undifferentiated cells (Fig. 8a), completely different components were utilized by the cells induced differentiation, either into TROMA-I-positive cells resembling extra-embryonic endoderm (SR96; Fig. 8b) or into neural cells expressing neural specific class III β-tubulin (IR96; Fig. 8c). During endodermal differentiation cyclin D2, cyclin D3 and p27 were also induced but they associated mainly with CDK4 (and only to a small extent with CDK6), thus forming inactive, predominantly cytoplasmic cyclin D2/D3–CDK4–p27 complexes, which replaced nuclear cyclin D1–CDK4 complexes contained in undifferentiated P19 cells. Differentiation towards neural lineage was also associated with up-regulation of D-type cyclins and p27, which then bound to CDK4 (and not CDK6). Notably, cyclins D1 and D2 were dominant in neural differentiation, instead of cyclins D2 and D3, typical of endodermal differentiation. Cyclin D2 is expressed throughout embryonic and adult brain (Ross & Riskin 1994; Ross *et al*. 1996) and its specific role in neurodifferentiation has been documented in several lines of evidence. Cyclin D2-deficient mice display defects in architecture of the cerebellum, due to inappropriate proliferation of granule cell precursors and due to defects in differentiation of granule and stellate interneurones (Huard *et al*. 1999). Moreover, additional

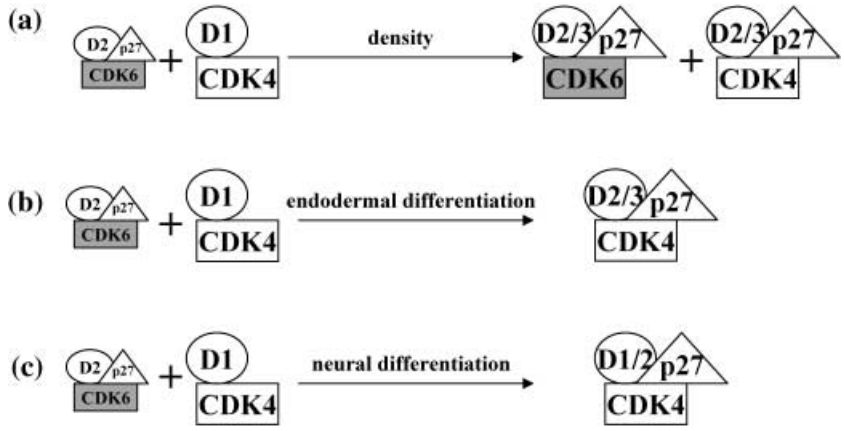

Figure 8. Shuffling of cyclin D–CDK4/6–p27 complexes in P19 EC cells. In exponentially growing P19 EC cells, kinase-active cyclin D1–CDK4 was a predominant complex but low amounts of cyclin D2–CDK6–p27 were also present. (a) When cells became confluent, cyclin D1 was down-regulated, and increased cyclins D2 and D3 together with p27 bound to CDK6 and to CDK4. (b) During endodermal differentiation, levels of cyclins D2 and D3 were increased and they formed kinase-inactive complexes with p27 and CDK4. (c) During differentiation into neural lineage, p27 and CDK4 bound to cyclins D1 and D2 and formed kinase-inactive cyclin D1/2–CDK4–p27 complexes.

ablation of cyclin D1 further amplifies the defects observed in cyclin D2-deficient mice – the cyclin D1–/–D2–/– mouse has severely impaired development of the cerebellum which develops only in a rudimentary form (Ciemerych *et al*. 2002). Cooperation of cyclins D1 and D2 thus correspond well with their specific up-regulation observed here in neural IR cells.

Two major conclusions can be drawn from the above analysis: (i) distinct D-type cyclins are utilized in neural and endodermal differentiation; (ii) CDK4 is a major partner of D-type cyclins and p27 in differentiated cells, whereas CDK6 is bound to D-type cyclins and p27 in undifferentiated cells at higher densities. CDK4 and CDK6 are considered to be largely redundant in their ability to bind D-type cyclins and to phosphorylate target proteins, as well as in their biological function (for review, see Ekholm & Reed 2000). Distinct roles for CDK4 and CDK6 in cells of embryonic origin are suggested in our study, by differing metabolism of CDK4- and CDK6-containing complexes. We have shown previously that similar rapid and complete re-structuring of cyclin D–CDK4/6 complexes from cyclin D2/D3–CDK6 to cyclin D3–CDK4–p21/p27 accompanies fibroblast growth factor 2 (FGF2)-induced inhibition of cell proliferation in rat chondrosarcoma chondrocytes (Krejci *et al*. 2004). Furthermore, cyclin D3–CDK6 and cyclin D1–CDK4 complexes, which are typical for undifferentiated mESCs (Faast *et al*. 2004; Čajánek unpublished), become rebuilt into cyclin D3–CDK4–p27 complexes (Savatier *et al*. 1995; Bryja *et al*. 2004b) upon entry into the differentiation pathway. Unfortunately, functional significance of such dramatic molecular changes occurring to CDK4 and CDK6 is as yet largely unexplored, with only some distinct properties of CDK4 and CDK6 being recently found with respect to (i) substrate specificity (Takaki *et al*. 2005); (ii) sensitivity to the CKI inhibitors of INK4 family (Lin *et al*. 2001; Faast *et al*. 2004); and (iii) utilization of individual post-translational variants of p27 and subsequently ability to sequester p27 from CDK2. Although our experiments could not provide thorough functional analysis, they are still important by not only presenting further evidence for unequal roles of CDK4 and CDK6, but also primarily by pointing to CDK4, CDK6, and their partners concerning molecules that are involved in driving differentiation processes which take place in early development.

Here, we have demonstrated that individual D-type cyclins were differently utilized during lineage specification, with cyclins D1 and D2 (but not cyclin D3) being typical for differentiation towards the neural lineage. Similarly, substrate specificities of CDK4 and CDK6, and also CDK4 complexed to different D-type cyclins, may differ in substrate specificity as clearly demonstrated by Paternot *et al*. (2006). Cyclins D1 and D2 are crucial for neural development in mouse (Ciemerych *et al*. 2002) and cooperation of cyclins D1 and D2 in mouse development thus correspond well with their specific up-regulation observed here in neural lineage (IR) cells. Although the precise molecular mechanism of cyclin D1 and/or cyclin D2 action in neurodifferentiation is not yet known, recent data suggest that both these cyclins may be involved in regulation of apoptosis in neural cells. Cyclin D2 has been shown to mediate anti-apoptotic effects on cerebellar neuroblasts (Poguet *et al*. 2003) and cytoplasmic localization of cyclin D1 is required to protect differentiating neurones from apoptosis (Sumrejkanchanakij *et al*. 2003). We have previously demonstrated similar anti-apoptotic functions for cyclin D3 in complex with p27 in mESCs, differentiating into extra-embryonic endoderm (SR cells) (Bryja *et al*. 2004b). We suggest that neural IR cells expressing high levels of cyclins D1 and D2 localized in the cytoplasm, bound to but not activating CDK4, provide an *in vitro* system to investigate the role of D-type cyclins in neural differentiation in more detail.

In summary, our data provide evidence that depending on cell fate, diverse cyclin D–CDK4/6–p27 complexes are formed and are utilized distinctly by pluripotent embryonic cells. Whereas CDK4 is a major partner of cytoplasmic D-type cyclins and p27 in differentiating cells (associated with cyclins D1 and D2 in neuroectodermal cells and with cyclins D2 and D3 in endodermal cells), CDK6 binds D-type cyclins and p27 when cells are at high cell density. Our data suggest that individual D-type cyclins as well as CDK4 and CDK6 have sub-type specific and cell cycle regulation-independent functions utilized during embryonic development and differentiation of stem cells. From a practical point of view, this study provides a well-characterized experimental model to address biological processes whose understanding is required for safe use of human ES cells in cell therapies.

ACKNOWLEDGEMENTS

We are very grateful to Dr. J. Lukas and Dr. P. Draber for providing us with antibodies, and to Mrs Iveta Nevriva and Mrs Johana Maresova for excellent technical assistance. This research was supported by the Academy of Sciences of the Czech Republic (AV0Z50390512, AV0Z50390703, 1QS500040507, AVOZ50040507, AVOZ50040702), by the Grant Agency of the Czech Republic (524/03/P171, 301/05/0463, 204/07/0834), and by the Ministry of Education, Youth and Sports of the Czech Republic (1M0021620803, MSM0021622430, 1M0538).

REFERENCES

Andäng M, Hjerling-Leffler J, Moliner A, Lundgren TK, Castelo-Branco G, Nanou E, Pozas E, Bryja V, Halliez S, Nishimaru H, Wilbertz J, Arenas E, Koltzenburg M, Charnay P, El Manira A, Ibañez CF, Ernfors P (2008) Histone H2AX-dependent $GABA_A$ receptor regulation of stem cell proliferation. *Nature* **451**, 460–464.

Andrews PW, Przyborski SA, Thomson JA (2001) Embryonal carcinoma cells as embryonic stem cells. In: Marshak DR, Gardner RL, Gottlieb D, eds. *Stem Cell Biology*, pp. 231–265. New York: Cold Spring Harbor Laboratory Press.

Baldassarre G, Barone MV, Belleti B, Sandomenico C, Bruni P, Spiezia S, Boccia A, Vento MT, Romano A, Pepe S,

Fusco A, Viglietto G (1999) Key role of the cyclin-dependent kinase inhibitor $p27^{kip1}$ for embryonal carcinoma cell survival and differentiation. *Oncogene* **18**, 6241–6251.

Baldassarre G, Boccia A, Bruni P, Sandomenico C, Barone MV, Pepe S, Angrisano T, Belletti B, Motti ML, Fusco A, Viglietto G (2000) Retinoic acid induces neuronal differentiation of embryonal carcinoma cells by reducing proteasome-dependent proteolysis of the cyclin-dependent inhibitor p27. *Cell Growth Differ*. **11**, 517–526.

Bartkova J, Lukas J, Muller H, Strauss M, Gusterson B, Bartek J (1995) Abnormal patterns of D-type cyclin expression and G_1 regulation in human head and neck cancer. *Cancer Res*. **55**, 949–956.

Bartkova J, Zemanova M, Bartek J (1996) Abundance and subcellular localisation of cyclin D3 in human tumours. *Int. J. Cancer* **65**, 323–327.

Bryja V, Cajanek L, Pachernik J, Hall AC, Horvath V, Dvorak P, Hampl A (2005) Abnormal development of mouse embryoid bodies lacking $p27^{kip1}$ cell cycle regulator. *Stem Cells* **23**, 965–974.

Bryja V, Pachernik J, Faldikova L, Krejci P, Pogue R, Nevriva I, Dvorak P, Hampl A (2004a) The role of p27(Kip1) in maintaining the levels of D-type cyclins *in vivo*. *Biochim. Biophys. Acta* **1691**, 105–116.

Bryja V, Pachernik J, Soucek K, Horvath V, Dvorak P, Hampl A (2004b) Increased apoptosis in differentiating p27-deficient mouse embryonic stem cells. *Cell Mol. Life Sci*. **61**, 1384–1400.

Chellappan SP, Giordano A, Fisher PB (1998) Role of cyclin-dependent kinases and their inhibitors in cellular differentiation and development. *Curr. Top. Microbiol. Immunol*. **227**, 57–103.

Ciemerych MA, Kenney AM, Sicinska E, Kalasczynska I, Bronson RT, Rowitch DH, Gardner H, Sicinski P (2002) Development of mice expressing a single D-type cyclin. *Genes Dev*. **16**, 3277–3289.

Ekholm SV, Reed SI (2000) Regulation of G(1) cyclin-dependent kinases in the mammalian cell cycle. *Curr. Opin. Cell Biol*. **12**, 676–684.

Faast R, White J, Cartwright P, Crocker L, Sarcevic B, Dalton S (2004) Cdk6-cyclin D3 activity in murine ES cells is resistant to inhibition by $p16^{INK4a}$. *Oncogene* **23**, 491–502.

Fantl V, Stamp G, Andrews A, Rosewell I, Dickson C (1995) Mice lacking cyclin D1 are small and show defects in eye and mammary gland development. *Genes Dev*. **9**, 2364–2372.

Gao CY, Zelenka P (1997) Cyclins, cyclin-dependent kinases and differentiation. *Bioessays* **19**, 307–315.

Gill MR, Slack R, Kiess M, Hamel PA (1998) Regulation of expression and activity of distinct pRB, E2F, D-type cyclin, and CKI family members during terminal differentiation of P19 cells. *Exp. Cell Res*. **244**, 157–170.

Glozak MA, Rogers MB (2001) Retinoic acid- and bone morphogenetic protein 4-induced apoptosis in P19 embryonal carcinoma cells requires p27. *Exp. Cell Res*. **268**, 128–138.

Huard JMT, Forster CC, Carter ML, Sicinski P, Ross ME (1999) Cerebellar histogenesis is disturbed in mice lacking cyclin D2. *Development* **126**, 1927–1935.

Jirmanova L, Bulavin DV, Fornace AJ Jr (2005) Inhibition of the ATR/Chk1 pathway induces a p38-dependent S-phase delay in mouse embryonic stem cells. *Cell Cycle* **4**, 1428–1434.

Kozar K, Ciemerych MA, Rebel VI, Shigematsu H, Zagozdzon A, Sicinska E, Geng Y, Yu Q, Bhattacharya S, Bronson RT, Akashi K, Sicinski P (2004) Mouse development and cell proliferation in the absence of D-cyclins. *Cell* **118**, 477–491.

Krejci P, Bryja V, Pachernik J, Hampl A, Pogue R, Mekikian P, Wilcox WR (2004) FGF2 inhibits proliferation and alters the cartilage-like phenotype of RCS cells. *Exp. Cell Res*. **297**, 152–164.

Li Y, Glozak MA, Smith SM, Rogers MB (1999) The expression and activity of D-type cyclins in F9 embryonal carcinoma cells: modulation of growth by RXR-selective retinoids. *Exp. Cell Res*. **253**, 372–384.

Lin J, Jinno S, Okayama H (2001) Cdk6-cyclin D3 complex evades inhibition by inhibitor proteins and uniquely controls cell's proliferation competence. *Oncogene* **20**, 2000–2009.

Livak KJ, Schmittgen TD (2001) Analysis of relative gene expression data using real-time quantitative PCR and the 2(-Delta Delta C(T)) Method. *Methods* **25**, 402–408.

Malumbres M, Sotillo R, Santamaria D, Galan J, Cerezo A, Ortega S, Dubus P, Barbacid M (2004) Mammalian cells cycle without the D-type cyclin-dependent kinases Cdk4 and Cdk6. *Cell* **118**, 493–504.

Nakayama K, Nakayama K (1998) Cip/Kip cyclin-dependent kinase inhibitors: brakes of the cell cycle engine during development. *Bioessays* **20**, 1020–1029.

Pachernik J, Bryja V, Esner M, Kubala L, Dvorak P, Hampl A (2005) Neural differentiation of pluripotent mouse embryonal carcinoma cells by retinoic acid: inhibitory effect of serum. *Physiol. Res*. **54**, 115–122.

Paternot S, Arsenijevic T, Coulonval K, Bockstaele L, Dumont JE, Roger PP (2006) Distinct specificities of pRb phosphorylation by CDK4 activated by cyclin D1 or cyclin D3: differential involvement in the distinct mitogenic modes of thyroid epithelial cells. *Cell Cycle* **5**, 61–70.

Poguet A-L, Legrand C, Feng X, Yen PM, Meltzer P, Samarut J, Flamant F (2003) Microarray analysis of knockout mice identifies cyclin D2 as a possible mediator for the action of thyroid hormone during the postnatal development of the cerebellum. *Dev. Biol*. **254**, 188–199.

Preclikova H, Bryja V, Pachernik J, Krejci P, Dvorak P, Hampl A (2002) Early cycling-independent changes to p27, cyclin D2, and cyclin D3 in differentiating mouse embryonal carcinoma cells. *Cell Growth Differ*. **13**, 421–430.

Ross ME, Carter ML, Lee JH (1996) MN20, a D2 cyclin, is transiently expressed in selected neural populations during embryogenesis. *J. Neurosci*. **16**, 210–219.

Ross ME, Riskin M (1994) MN20, a D2 cyclin found in brain, is implicated in neural differentiation. *J. Neurosci*. **14**, 6384–6391.

Savatier P, Lapillonne H, van Grunsven LA, Rudkin BB, Samarut J (1995) Withdrawal of differentiation inhibitory activity/leukemia inhibitory factor up-regulates D-type cyclins and cyclin-dependent kinase inhibitors in mouse embryonic stem cells. *Oncogene* **12**, 309–322.

Sherr CJ (1995) D-type cyclins. *Trends Biochem. Sci*. **20**, 187–190.

Sherr CJ, Roberts JM (1999) CDK inhibitors: positive and negative regulators of G_1-phase progression. *Genes Dev*. **13**, 1501–1512.

Sicinski P, Donaher JL, Parker SB, Li T, Fazeli A, Gardner H, Haslam SZ, Bronson RT, Elledge SJ, Weinberg RA (1995) Cyclin D1 provides a link between development and oncogenesis in the retina and breast. *Cell* **82**, 621–630.

Slee EA, Adrain C, Martin SJ (2001) Executioner caspase-3-6, and -7 perform distinct, non-redundant roles during the demolition phase of apoptosis. *J. Biol. Chem*. **276**, 7320–7326.

Smith A (2001) Embryonic stem cells. In: Marshak DR, Gardner RL, Gottlieb D, eds. *Stem Cell Biology*, pp. 205–230. New York: Cold Spring Harbor Laboratory Press.

Sumrejkanchanakij P, Tamamori-Adachi M, Matsunaga Y, Eto K (2003) Role of cyclin D1 cytoplasmic sequestration in the survival of postmitotic neurons. *Oncogene* **22**, 8723–8730.

Takaki T, Fukasawa K, Suzuki-Takahashi I, Semba K, Kitagawa M, Taya Y, Hirai H (2005) Preferences for phosphorylation sites in the retinoblastoma protein of D-type cyclin-dependent kinases, Cdk4 and Cdk6, *in vitro*. *J. Biochem. (Tokyo)* **137**, 381–386.

Watanabe Y, Watanabe T, Kitagawa M, Taya Y, Nakayama K, Motoyama N (1999) pRb phosphorylation is regulated differentially by cyclin-dependent kinase (Cdk) 2 and Cdk4 in retinoic acid-induced neuronal differentiation of P19 cells. *Brain Res*. **842**, 342–350.